Supplementary Information for:

A Maxwell-Based Dual-Morphology Wet Snow Microstructure Model for Liquid Water Amount Retrieval in Greenland's Percolation Zone Using SMAP L-Band Radiometry

Hui Jiang[1], Firoz Borah[1], Leung Tsang[1],
Zhenming Huang[1], Alamgir Hossan[2], and Andreas Colliander[3]

[1]Radiation Laboratory, Department of Electrical Engineering and Computer Science, University of Michigan, Ann Arbor, MI 48109, USA

[2]Jet Propulsion Laboratory, California Institute of Technology, La Cañada Flintridge, CA 91011, USA

[3]Finnish Meteorological Institute, Helsinki, 00560, Finland

This document is the Supplementary Information for the paper titled above. It gives the implementation details of the temporally constrained SMAP L-band retrieval algorithm and the post retrieval dry screening procedure. The notation follows the main paper. The index i denotes the SMAP pass index, j denotes the candidate index at a given SMAP pass, and $p \in \{v, h\}$ denotes polarization. The code variable `fv_w` is the same quantity as the liquid water volume fraction, denoted here as LWC. A representative sensitivity and ablation test is also provided in Sect. 10 to show how the retrieval responds to removal of the dry screening, removal of the weak SMAP TB shape prior, and perturbation of the main regularization weights.

1 Notation and mathematical operations

Several operations are used repeatedly in the retrieval equations. They are defined here so that the later formulas are self contained. For a scalar x and lower and upper bounds $a < b$, the clipping operation is

$$\mathrm{clip}_{[a,b]}(x) = \min\{\max(x, a), b\}. \tag{S1}$$

Thus $\mathrm{clip}_{[0,1]}(x)$ maps any value below 0 to 0 and any value above 1 to 1. When a vector or time series is used as the argument, Eq. (S1) is applied element by element. The notation

$$\mathrm{clip}[x, a, b] \equiv \mathrm{clip}_{[a,b]}(x) \tag{S2}$$

is used in a few equations for compactness. The operations $\max(x_1, x_2, \dots)$ and $\min(x_1, x_2, \dots)$ return the largest and smallest values among their arguments. The positive part of a scalar is denoted by

$$[x]_+ = \max(x, 0). \tag{S3}$$

For a seasonal sequence x_i, the normalization to the range $[0, 1]$ is

$$\mathcal{N}_{[0,1]}[x_i] = \frac{x_i - \min_i x_i}{\max_i x_i - \min_i x_i}. \tag{S4}$$

The symbol $P_q(x)$ denotes the qth percentile of the seasonal sequence x_i. The symbol $\mathrm{std}_5(x)_i$ denotes the standard deviation of x over a five pass moving window centered on pass i, with shortened windows near the beginning and end of the time series. The dry season robust scale is written as $1.4826\,\mathrm{MAD}$, where MAD is the median absolute deviation. The operator $\arg\min$ denotes the argument that minimizes the expression following it.

All weights w and ω are dimensionless tuning parameters that control the relative importance of different cost terms. All σ terms are normalization scales that make the corresponding residuals or penalties dimensionless. Their numerical values are listed in Tables S2 to S8.

2 Why the retrieval is formulated as a time series problem

Each SMAP pass provides two observations, TB_v and TB_h, but the wet snow state is described by three unknowns: the thin coated water fraction α, LWC, and the effective wet layer thickness d_{wet}. A single SMAP pass therefore cannot uniquely determine the wet state. The retrieval uses the information contained in the whole seasonal time series. The algorithm first constructs many locally acceptable wet candidates at each pass, then selects the lowest cost seasonal path through these candidates.

The retrieval is performed in two main stages.

1. A wet first time series retrieval is performed. In this stage every SMAP pass is allowed to be wet, so that weak but physically meaningful melt signals are not rejected too early.

2. A dry screening step is then applied to the preliminary wet solution. This step removes passes that are better interpreted as dry, especially after the main melt season when the absolute TB baseline may remain shifted from the January to April dry reference.

This two stage design is important. The wet first retrieval already contains terms that discourage wet solutions when the SMAP signal looks dry, but that is not always sufficient. After the wet season, especially in November, the snow and firn column can be physically dry while the observed brightness temperatures do not return exactly to the January to April mean. In the two layer radiative transfer model, such a shifted dry baseline can be mistakenly fitted by placing a small wet layer at the top. The dry screening step is introduced to remove this class of artificial weak wet solutions using polarization stability and morning evening diagnostics.

3 Candidate library and forward model

3.1 Candidate library

For each SMAP overpass i, the thin coated water fraction is divided into five ranges,

$$\begin{aligned}
&\alpha_{i,j} \in \mathcal{A}_k, \qquad k = 1, \ldots, 5, \\
&\mathcal{A}_1 = [0, 0.2), \qquad \mathcal{A}_2 = [0.2, 0.4), \qquad \mathcal{A}_3 = [0.4, 0.6), \\
&\mathcal{A}_4 = [0.6, 0.8), \qquad \mathcal{A}_5 = [0.8, 1.0], \\
&\mathbf{x}_{i,j} = (\alpha_{i,j}, \mathrm{LWC}_{i,j})\,.
\end{aligned} \tag{S5}$$

Here $\mathcal{A}_k$ is the kth prescribed α range, and $\mathbf{x}_{i,j}$ is the local candidate defined by α and LWC. Within each α range, multiple LWC values are generated. The purpose of using five α ranges is to make sure that the candidate library samples both compact Tri-C dominated states and thin coated, film like states. The wet layer thickness d_{wet} is not sampled as a third grid dimension. Instead, it is solved analytically for each (α, LWC) candidate.

For each candidate in Eq. (S5), the neural network permittivity emulator gives the complex effective permittivity $\epsilon_{r,i,j}$. This permittivity is then used in the two layer forward model.

3.2 Two layer radiative transfer model in linear attenuation form

For a fixed candidate $(\alpha_{i,j}, \text{LWC}_{i,j})$, the modeled brightness temperature can be written as

$$\begin{aligned}
\text{TB}^{\text{mod}}_{p,i,j} &= a_{p,i,j} + b_{p,i,j} E_{i,j}, \qquad p \in \{v, h\}, \\
a_{p,i,j} &= (1 - r_{p,i,j})\, T_{s,i}, \\
b_{p,i,j} &= (1 - r_{p,i,j}) \left(\text{TB}^{\text{dry}}_{p} - T_{s,i} \right), \\
E_{i,j} &= \exp\left[-\kappa_{a,i,j} d_{\text{wet},i,j} \sec(\theta) \right].
\end{aligned} \tag{S6}$$

In Eq. (S6), $T_{s,i}$ is the wet layer temperature, $\text{TB}^{\text{dry}}_{p}$ is the January to April mean dry season SMAP brightness temperature, $r_{p,i,j}$ is the Fresnel power reflectivity, $\kappa_{a,i,j}$ is the attenuation coefficient, $d_{\text{wet},i,j}$ is the wet layer thickness, and $\theta = 40^\circ$ is the SMAP incidence angle.

The reflectivities and attenuation coefficient in Eq. (S6) are computed from $\epsilon_{r,i,j}$ as

$$\begin{aligned}
k_0 &= 2\pi f \sqrt{\mu_0 \epsilon_0}, \qquad k_1 = k_0 \sqrt{\epsilon_{r,i,j}}, \\
\kappa_{a,i,j} &= 2\, \text{Im}(k_1), \\
k_z &= k_0 \cos\theta, \qquad k_{1z} = \sqrt{k_1^2 - k_0^2 \sin^2\theta}, \\
R_v &= \frac{\epsilon_{r,i,j} k_z - k_{1z}}{\epsilon_{r,i,j} k_z + k_{1z}}, \qquad R_h = \frac{k_z - k_{1z}}{k_z + k_{1z}}, \\
r_v &= |R_v|^2, \qquad r_h = |R_h|^2.
\end{aligned} \tag{S7}$$

Here $f = 1.4\,\text{GHz}$ is the SMAP frequency, μ_0 and ϵ_0 are the permeability and permittivity of free space, k_0 is the free space wavenumber, and k_1 is the complex effective wavenumber in the wet snow layer. The attenuation coefficient $\kappa_{a,i,j}$, and the power reflectivities r_v and r_h, are the quantities that enter Eq. (S6).

3.3 Analytical solution for wet layer thickness

For fixed α and LWC, Eq. (S6) is linear in the attenuation factor $E_{i,j}$. Before solving for $E_{i,j}$, the allowed wet layer thickness range is converted into attenuation factor limits,

$$E_{\min} = \exp\left[-\kappa_{a,i,j} d_{\max} \sec\theta \right], \qquad E_{\max} = \exp\left[-\kappa_{a,i,j} d_{\min} \sec\theta \right]. \tag{S8}$$

where $d_{\min}$ and $d_{\max}$ are the lower and upper bounds on wet layer thickness, and $\kappa_{a,i,j}$ is the attenuation coefficient defined in Eq. (S7).

The least squares attenuation factor for fitting both polarizations is

$$E^*_{i,j} = \text{clip}\left[\frac{\sum_{p=v,h} b_{p,i,j} \left(\text{TB}^{\text{obs}}_{p,i} - a_{p,i,j} \right)}{\sum_{p=v,h} b^2_{p,i,j}}, E_{\min}, E_{\max} \right]. \tag{S9}$$

Here $a_{p,i,j}$ and $b_{p,i,j}$ are defined in Eq. (S6), $\text{TB}^{\text{obs}}_{p,i}$ is the observed SMAP brightness temperature, $E_{\min}$ and $E_{\max}$ are defined in Eq. (S8), and the clipping operation is defined in Eq. (S1).

The optimal wet layer thickness is then

$$d^*_{\mathrm{wet},i,j} = -\frac{\ln\left(E^*_{i,j}\right)}{\kappa_{a,i,j}\sec\theta}. \tag{S10}$$

where $E^*_{i,j}$ is the optimized attenuation factor from Eq. (S9), and $\kappa_{a,i,j}$ is the attenuation coefficient from Eq. (S7). Finally, the candidate LWA is

$$\mathrm{LWA}_{i,j} = 1000\,\mathrm{LWC}_{i,j}\,d^*_{\mathrm{wet},i,j}, \tag{S11}$$

where $\mathrm{LWC}_{i,j}$ is the candidate liquid water volume fraction from Eq. (S5), and $d^*_{\mathrm{wet},i,j}$ is the optimized wet layer thickness from Eq. (S10). The factor 1000 converts meters of water equivalent to millimeters.

4 SMAP wetness indicators used by the retrieval

The retrieval uses several indicators derived from the SMAP time series. These indicators are not independent observations of LWA. They only tell the inversion whether the time series is behaving more like a wet state, a melt onset state, a freezing state, or a dry state with a shifted baseline.

4.1 Dry referenced TB anomaly and polarization departure

The dry referenced TB anomaly is

$$A_i^{\mathrm{TB}} = \frac{1}{2}\left[\max\left(\mathrm{TB}^{\mathrm{obs}}_{v,i} - \mathrm{TB}^{\mathrm{dry}}_{v}, 0\right) + \max\left(\mathrm{TB}^{\mathrm{obs}}_{h,i} - \mathrm{TB}^{\mathrm{dry}}_{h}, 0\right)\right], \tag{S12}$$

$$A_i = \mathrm{clip}_{[0,1]}\left(\frac{A_i^{\mathrm{TB}} - A_0}{A_{\mathrm{hi}} - A_0}\right). \tag{S13}$$

Here $\mathrm{TB}^{\mathrm{dry}}_{v}$ and $\mathrm{TB}^{\mathrm{dry}}_{h}$ are the January to April dry season references, $A_0 = 3\,\mathrm{K}$, and A_{hi} is the 85th percentile of the seasonal anomaly with a minimum value of $A_0 + 1\,\mathrm{K}$. The normalized anomaly A_i in Eq. (S13) is obtained from A_i^{TB} in Eq. (S12) using the clipping operator defined in Eq. (S1).

The normalized polarization ratio is

$$\mathrm{NPR}_i = \frac{\mathrm{TB}^{\mathrm{obs}}_{v,i} - \mathrm{TB}^{\mathrm{obs}}_{h,i}}{\mathrm{TB}^{\mathrm{obs}}_{v,i} + \mathrm{TB}^{\mathrm{obs}}_{h,i}}, \qquad \mathrm{NPR}^{\mathrm{dry}} = \frac{\mathrm{TB}^{\mathrm{dry}}_{v} - \mathrm{TB}^{\mathrm{dry}}_{h}}{\mathrm{TB}^{\mathrm{dry}}_{v} + \mathrm{TB}^{\mathrm{dry}}_{h}}. \tag{S14}$$

The normalized polarization departure is

$$\eta_i = \mathrm{clip}_{[0,1]}\left(\frac{|\mathrm{NPR}_i - \mathrm{NPR}^{\mathrm{dry}}| - \eta_0}{\eta_1 - \eta_0}\right), \tag{S15}$$

where NPR_i and $\mathrm{NPR}^{\mathrm{dry}}$ are defined in Eq. (S14), $\eta_0 = 0.012$, and $\eta_1 = 0.035$. A large η_i indicates that the polarization ratio departs from the dry season reference.

4.2 Rise, retreat, variability, and melt memory

The positive anomaly rise term and retreat term are

$$R_i = \mathcal{N}_{[0,1]}\left[\max(A_i - A_{i-1}, 0)\right], \qquad Q_i = \mathcal{N}_{[0,1]}\left[\max(A_{i-1} - A_i, 0)\right], \tag{S16}$$

where A_i is the normalized TB anomaly defined in Eq. (S13), and $\mathcal{N}_{[0,1]}[\cdot]$ is defined in Eq. (S4).

The local variability indicator is

$$V_i = \mathrm{clip}_{[0,1]}\left(0.40V_i^{\mathrm{TB}} + 0.35V_i^{\Delta\mathrm{TB}} + 0.25V_i^{\mathrm{NPR}}\right). \tag{S17}$$

Here V_i^{TB} is the activity from the moving window TB anomaly standard deviation, $V_i^{\Delta\mathrm{TB}}$ is the activity from the pass to pass TB jump, and V_i^{NPR} is the activity from the moving window NPR variability. Each of these three sub indicators is normalized to the range $[0, 1]$ using Eq. (S1).

The melt entry evidence is

$$\mathcal{E}_i^{\mathrm{enter}} = \mathrm{clip}_{[0,1]}\left(0.50\eta_i + 0.20R_i + 0.15A_i + 0.15V_i\right). \tag{S18}$$

where η_i is the polarization departure defined in Eq. (S15), R_i is the anomaly rise term defined in Eq. (S16), A_i is the normalized TB anomaly defined in Eq. (S13), and V_i is the local variability indicator defined in Eq. (S17).

The melt memory is updated as

$$M_i = \max\left[\mathcal{E}_i^{\mathrm{enter}}, \exp\left(-\frac{\Delta t_i}{\tau_M}\right)M_{i-1}\right], \qquad \tau_M = 8\,\mathrm{d}. \tag{S19}$$

where $\mathcal{E}_i^{\mathrm{enter}}$ is the entry evidence defined in Eq. (S18), M_{i-1} is the previous melt memory value, and Δt_i is the time interval between passes $i-1$ and i.

The wet evidence is

$$\mathcal{E}_i^{\mathrm{wet}} = \mathrm{clip}_{[0,1]}\left(0.45\eta_i + 0.25M_i + 0.15A_i + 0.15V_i\right). \tag{S20}$$

where η_i, M_i, A_i, and V_i are defined in Eqs. (S15), (S19), (S13), and (S17), respectively.

The wet admission index is

$$\mathcal{W}_i^{\mathrm{wet}} = \max\left(\mathcal{E}_i^{\mathrm{enter}}, \mathcal{E}_i^{\mathrm{wet}}, \eta_i, V_i\right). \tag{S21}$$

where $\mathcal{E}_i^{\mathrm{enter}}$, $\mathcal{E}_i^{\mathrm{wet}}$, η_i, and V_i are defined in Eqs. (S18), (S20), (S15), and (S17). The index is large when the time series provides evidence that a wet solution is plausible.

A stable dry indicator and a freezing indicator are also used:

$$\mathcal{S}_i^{\mathrm{dry}} = \mathrm{clip}_{[0,1]}\left[(0.30 + 0.70A_i)(1-\eta_i)^{1.35}(1-V_i)^{1.10}(0.35 + 0.65(1-M_i))\right], \tag{S22}$$

$$\mathcal{F}_i = \mathrm{clip}_{[0,1]}\left[(0.45\mathcal{S}_i^{\mathrm{dry}} + 0.30Q_i + 0.25(1-M_i))(0.20 + 0.80A_i)\right]. \tag{S23}$$

In Eq. (S22), A_i, η_i, V_i, and M_i are defined in Eqs. (S13), (S15), (S17), and (S19). In Eq. (S23), $\mathcal{S}_i^{\mathrm{dry}}$ is defined in Eq. (S22), Q_i is the retreat term from Eq. (S16), and A_i and M_i are defined in Eqs. (S13) and (S19).

4.3 SMAP TB shape function for the weak LWA prior

The normalized SMAP TB shape function is

$$S_i^{\mathrm{TB}} = \frac{A_i^{\mathrm{TB}} - \min_i A_i^{\mathrm{TB}}}{\max_i A_i^{\mathrm{TB}} - \min_i A_i^{\mathrm{TB}}}. \tag{S24}$$

where A_i^{TB} is the dry referenced TB anomaly defined in Eq. (S12). The shape function is used only as a weak seasonal guide. It does not convert TB into an independent LWA measurement.

In the implementation, a weak LWA scale target is also constructed from the wet indicators. The wet strength is

$$\mathcal{W}_i^{\mathrm{str}} = \max\left(\mathcal{E}_i^{\mathrm{wet}}, 0.75\mathcal{E}_i^{\mathrm{enter}}, 0.60V_i\right), \tag{S25}$$

where $\mathcal{E}_i^{\mathrm{wet}}$, $\mathcal{E}_i^{\mathrm{enter}}$, and V_i are defined in Eqs. (S20), (S18), and (S17). The reference wet depth is

$$d_i^{\mathrm{ref}} = \mathrm{clip}_{[0.03,4.0]}\left(0.04 + 0.22\mathcal{W}_i^{\mathrm{str}} + 2.00M_i\right), \tag{S26}$$

where $\mathcal{W}_i^{\mathrm{str}}$ is defined in Eq. (S25), and M_i is the melt memory defined in Eq. (S19). The soft LWC scale is

$$\mathrm{LWC}_i^{\mathrm{soft}} = \mathrm{clip}_{[0.001,0.030]}\left(0.001 + 0.010\eta_i + 0.008M_i + 0.004V_i\right), \tag{S27}$$

where η_i, M_i, and V_i are defined in Eqs. (S15), (S19), and (S17). The weak LWA target is

$$\mathrm{LWA}_i^{\mathrm{shape}} = 1000\, d_i^{\mathrm{ref}} \max\left(\mathrm{LWC}_i^{\mathrm{soft}}, 0.001\right). \tag{S28}$$

where d_i^{ref} is defined in Eq. (S26), and $\mathrm{LWC}_i^{\mathrm{soft}}$ is defined in Eq. (S27). The main paper writes this weak target compactly as $L_{\mathrm{shape}}S_i^{\mathrm{TB}}$.

5 Local candidate cost function

This section defines the local cost terms. The terms are first defined individually. The full implementation cost is then given after all of its components have been introduced.

The two polarization TB misfit is

$$J_{i,j}^{\mathrm{TB}} = \left[\frac{\mathrm{TB}_{v,i,j}^{\mathrm{mod}} - \mathrm{TB}_{v,i}^{\mathrm{obs}}}{\sigma_T}\right]^2 + \left[\frac{\mathrm{TB}_{h,i,j}^{\mathrm{mod}} - \mathrm{TB}_{h,i}^{\mathrm{obs}}}{\sigma_T}\right]^2. \tag{S29}$$

where $\mathrm{TB}_{v,i,j}^{\mathrm{mod}}$ and $\mathrm{TB}_{h,i,j}^{\mathrm{mod}}$ are modeled brightness temperatures from Eq. (S6), evaluated using the optimized thickness from Eq. (S10). The scale σ_T is listed in Table S2.

The weak SMAP TB shape penalty is

$$J_{i,j}^{\mathrm{shape}} = \left[\frac{\mathrm{LWA}_{i,j} - \mathrm{LWA}_i^{\mathrm{shape}}}{\sigma_{\mathrm{shape}}}\right]^2. \tag{S30}$$

where $\mathrm{LWA}_{i,j}$ is the candidate LWA defined in Eq. (S11), and $\mathrm{LWA}_i^{\mathrm{shape}}$ is the weak LWA target defined in Eq. (S28).

The wet admissibility penalty is

$$J_{i,j}^{\mathrm{adm}} = \left[\frac{\max(\mathcal{W}_{\mathrm{min}} - \mathcal{W}_i^{\mathrm{wet}}, 0)}{\sigma_{\mathrm{adm}}}\right]^2, \qquad \mathcal{W}_{\mathrm{min}} = 0.24. \tag{S31}$$

where $\mathcal{W}_i^{\mathrm{wet}}$ is the wet admission index defined in Eq. (S21). This term penalizes a wet candidate only when the time series evidence for wet snow is weak.

A dry explanation penalty is used to suppress weak artificial wet solutions when a dry interpretation fits almost as well. Let

$$G_{i,j}^{\mathrm{fit}} = J_i^{\mathrm{dryfit}} - J_{i,j}^{\mathrm{TB}}, \qquad D_i^{\mathrm{fit}} = \frac{1}{1 + J_i^{\mathrm{dryfit}}/\sigma_{\mathrm{drygood}}}. \tag{S32}$$

where J_i^{dryfit} is the TB fitting cost of a dry upper layer, and $J_{i,j}^{\text{TB}}$ is the TB misfit defined in Eq. (S29). The quantity $G_{i,j}^{\text{fit}}$ measures how much the wet candidate improves the fit over the dry fit.

The dry suppression factor is

$$\mathcal{D}_i^{\text{sup}} = \text{clip}_{[0,1]}\left[\max(\mathcal{S}_i^{\text{dry}}, 1 - \mathcal{W}_i^{\text{wet}})\right]. \tag{S33}$$

where $\mathcal{S}_i^{\text{dry}}$ is the stable dry indicator defined in Eq. (S22), and $\mathcal{W}_i^{\text{wet}}$ is the wet admission index defined in Eq. (S21). The dry explanation penalty is

$$J_{i,j}^{\text{dry}} = D_i^{\text{fit}}\,\mathcal{D}_i^{\text{sup}}\left[\frac{\max(G_{\min} - G_{i,j}^{\text{fit}}, 0)}{\sigma_{\text{drygain}}}\right]^2, \qquad G_{\min} = 0.60. \tag{S34}$$

where D_i^{fit} and $G_{i,j}^{\text{fit}}$ are defined in Eq. (S32), and $\mathcal{D}_i^{\text{sup}}$ is defined in Eq. (S33).

The low water factor is

$$\ell_{i,j} = \text{clip}_{[0,1]}\left(\frac{\text{LWC}_{\text{low}} - \text{LWC}_{i,j}}{\text{LWC}_{\text{low}}}\right), \qquad \text{LWC}_{\text{low}} = 0.006. \tag{S35}$$

where $\text{LWC}_{i,j}$ is the candidate LWC in Eq. (S5). The dry like dielectric factor is

$$\mathcal{D}_{i,j}^{\epsilon} = \frac{1}{1 + (\epsilon_{\text{sep},i,j})^2}, \qquad \epsilon_{\text{sep},i,j} = \left[\left(\frac{\text{Re}\epsilon_{i,j} - \text{Re}\epsilon_i^{\text{dry}}}{0.12}\right)^2 + \left(\frac{\text{Im}\epsilon_{i,j} - \text{Im}\epsilon_i^{\text{dry}}}{0.010}\right)^2\right]^{1/2}. \tag{S36}$$

where $\epsilon_{i,j}$ is the candidate effective permittivity from the neural network emulator, and ϵ_i^{dry} is the dry snow permittivity used for the dry fit.

The stable dry and dry like penalties are

$$J_{i,j}^{\text{stable}} = (\mathcal{S}_i^{\text{dry}})^{1.1}\left\{\ell_{i,j}\left[\left(\frac{\alpha_{i,j}}{\sigma_{\alpha,\text{stable}}}\right)^2 + \left(\frac{d_{\text{wet},i,j}^*}{\sigma_{d,\text{stable}}}\right)^2\right] + \left(\frac{\text{LWA}_{i,j}}{\sigma_{\text{LWA,stable}}}\right)^2\right\}, \tag{S37}$$

$$J_{i,j}^{\text{drylike}} = \mathcal{S}_i^{\text{dry}}\,\ell_{i,j}\,\mathcal{D}_{i,j}^{\epsilon}\left[\frac{\max(G_{\text{film}} - G_{i,j}^{\text{fit}}, 0)}{\sigma_{\text{drylike}}}\right]^2. \tag{S38}$$

In Eqs. (S37) and (S38), $\mathcal{S}_i^{\text{dry}}$ is defined in Eq. (S22), $\ell_{i,j}$ is defined in Eq. (S35), $d_{\text{wet},i,j}^*$ is defined in Eq. (S10), $\text{LWA}_{i,j}$ is defined in Eq. (S11), $G_{i,j}^{\text{fit}}$ is defined in Eq. (S32), and $\mathcal{D}_{i,j}^{\epsilon}$ is defined in Eq. (S36).

The high LWC, prior, edge, depth cap, and tail penalties are

$$J_{i,j}^{\text{high}} = \left[\frac{\max(\text{LWC}_{i,j} - \text{LWC}_i^{\text{soft}}, 0)}{\sigma_{\text{LWC}}} \right]^2, \tag{S39}$$

$$J_{i,j}^{\alpha} = \left[\frac{\alpha_{i,j} - \alpha_i^{\text{prior}}}{\sigma_\alpha} \right]^2, \tag{S40}$$

$$J_{i,j}^{d} = \left[\frac{d_{\text{wet},i,j}^{*} - d_i^{\text{prior}}}{\sigma_d} \right]^2, \tag{S41}$$

$$J_{i,j}^{\text{edge}} = \left[\frac{\alpha_{i,j}}{\alpha_{\max}} \right]^q, \qquad \alpha_{\max} = 1.0, \tag{S42}$$

$$J_{i,j}^{\text{cap}} = \left[\frac{\max(d_{\text{wet},i,j}^{*} - d_i^{\text{cap}}, 0)}{\sigma_{\text{cap}}} \right]^2. \tag{S43}$$

In Eq. (S39), $\text{LWC}_i^{\text{soft}}$ is defined in Eq. (S27). In Eqs. (S40) and (S41), α_i^{prior} and d_i^{prior} are weak candidate class priors. In Eq. (S41) and Eq. (S43), $d_{\text{wet},i,j}^{*}$ is defined in Eq. (S10). The edge term in Eq. (S42) is only a soft numerical penalty that discourages solutions from lying exactly at the edge of the sampled α interval; no LWC dependent α cap is imposed.

The tail LWA cap is

$$\text{LWA}_i^{\text{tail}} = 0.6 + 4.5\mathcal{E}_i^{\text{enter}} + 3.0\eta_i + 2.0V_i. \tag{S44}$$

where $\mathcal{E}_i^{\text{enter}}$ is defined in Eq. (S18), η_i is defined in Eq. (S15), and V_i is defined in Eq. (S17). The late season tail penalty is

$$J_{i,j}^{\text{tail}} = \left[\max(\mathcal{F}_i, 0.75\mathcal{S}_i^{\text{dry}}) \right]^2 \left[\frac{\max(\text{LWA}_{i,j} - \text{LWA}_i^{\text{tail}}, 0)}{\sigma_{\text{tail}}} \right]^2. \tag{S45}$$

where $\mathcal{F}_i$ is the freezing indicator defined in Eq. (S23), $\mathcal{S}_i^{\text{dry}}$ is the stable dry indicator defined in Eq. (S22), $\text{LWA}_{i,j}$ is the candidate LWA defined in Eq. (S11), and $\text{LWA}_i^{\text{tail}}$ is the tail cap defined in Eq. (S44).

After all components have been defined, the implementation local cost is written as

$$\begin{aligned} J_{i,j}^{\text{loc}} &= w_{T,i} J_{i,j}^{\text{TB}} + w_{\text{shape}} J_{i,j}^{\text{shape}} + w_{\text{adm}} J_{i,j}^{\text{adm}} + w_{\text{dry}} J_{i,j}^{\text{dry}} + w_{\text{stable}} J_{i,j}^{\text{stable}} + w_{\text{drylike}} J_{i,j}^{\text{drylike}} \\ &\quad + w_{\text{high}} J_{i,j}^{\text{high}} + w_\alpha J_{i,j}^{\alpha} + w_d J_{i,j}^{d} + w_{\text{mode}} J_{i,j}^{\text{mode}} + w_{\text{edge}} J_{i,j}^{\text{edge}} + w_{\text{cap}} J_{i,j}^{\text{cap}} + w_{\text{tail}} J_{i,j}^{\text{tail}}. \end{aligned} \tag{S46}$$

where the individual terms are defined in Eqs. (S29), (S30), (S31), (S34), (S37), (S38), and (S39) to (S45). The main paper groups these implementation terms into the compact local cost shown in Section 3.3.

6 Dynamic programming and temporal coupling

The directional term used in the temporal transition cost is

$$J_i^{\text{dir}} = \begin{cases} \omega_{\text{dir}} \left[\dfrac{\max(-\Delta\text{LWA}_i, 0)}{\sigma_{\text{dir}}} \right]^2, & \Delta\mathcal{E}_i^{\text{wet}} > \delta_{\text{wet}}, \\ \omega_{\text{dir}} \left[\dfrac{\max(\Delta\text{LWA}_i, 0)}{\sigma_{\text{dir}}} \right]^2, & \Delta\mathcal{E}_i^{\text{wet}} < -\delta_{\text{wet}}, \\ 0, & |\Delta\mathcal{E}_i^{\text{wet}}| \le \delta_{\text{wet}}. \end{cases} \tag{S47}$$

where $\Delta\mathrm{LWA}_i = \mathrm{LWA}_i - \mathrm{LWA}_{i-1}$, $\Delta\mathcal{E}_i^{\mathrm{wet}} = \mathcal{E}_i^{\mathrm{wet}} - \mathcal{E}_{i-1}^{\mathrm{wet}}$, and $\mathcal{E}_i^{\mathrm{wet}}$ is defined in Eq. (S20). If the SMAP wet evidence increases, Eq. (S47) penalizes a decrease in LWA; if the wet evidence decreases, it penalizes an increase in LWA.

The late season transition penalty is

$$J_i^{\mathrm{freeze}} = \omega_{\mathrm{freeze}} \left[\max(\mathcal{F}_i, \mathcal{S}_i^{\mathrm{dry}})\right]^2 \left[\frac{\max(\mathrm{LWA}_i - \mathrm{LWA}_i^{\mathrm{tail}}, 0)}{\sigma_{\mathrm{freeze}}}\right]^2. \tag{S48}$$

where $\mathcal{F}_i$ is defined in Eq. (S23), $\mathcal{S}_i^{\mathrm{dry}}$ is defined in Eq. (S22), and $\mathrm{LWA}_i^{\mathrm{tail}}$ is defined in Eq. (S44).

For wet to wet transitions, the total transition cost is

$$J_{i-1,i}^{\mathrm{tr}} = \omega_\alpha \left[\frac{\alpha_i - \alpha_{i-1}}{\sigma_{\Delta\alpha}}\right]^2 + \omega_{\mathrm{LWC}} \left[\frac{\mathrm{LWC}_i - \mathrm{LWC}_{i-1}}{\sigma_{\Delta\mathrm{LWC}}}\right]^2 + \omega_d \left[\frac{d_{\mathrm{wet},i} - d_{\mathrm{wet},i-1}}{\sigma_{\Delta d}}\right]^2 + \omega_{\mathrm{LWA}} \left[\frac{\mathrm{LWA}_i - \mathrm{LWA}_{i-1}}{\sigma_{\Delta\mathrm{LWA}}}\right]^2 + \omega_m P_{i-1,i} + J_i^{\mathrm{dir}} + J_i^{\mathrm{freeze}}. \tag{S49}$$

where $P_{i-1,i}$ is a penalty for abrupt switching between very different candidate classes, J_i^{dir} is defined in Eq. (S47), and J_i^{freeze} is defined in Eq. (S48). The state variables α_i, LWC_i, $d_{\mathrm{wet},i}$, and LWA_i are the values of the candidate selected at pass i.

The preliminary wet seasonal path is then selected by dynamic programming,

$$\widehat{j}_{1:N} = \arg\min_{j_1,\ldots,j_N} \left[\sum_{i=1}^{N} J_{i,j_i}^{\mathrm{loc}} + \sum_{i=2}^{N} J_{i-1,i}^{\mathrm{tr}}(j_{i-1}, j_i)\right]. \tag{S50}$$

where J_{i,j_i}^{loc} is the local cost defined in Eq. (S46), and $J_{i-1,i}^{\mathrm{tr}}$ is the transition cost defined in Eq. (S49). The dynamic programming step selects the lowest cost seasonally coherent path rather than the lowest cost candidate at each pass independently.

7 Post retrieval dry screening

7.1 Why the dry screening is needed

The wet first retrieval is intentionally permissive. It avoids rejecting weak melt signals at onset and during late season refreezing. However, the wet first stage is not enough to remove all dry passes. The reason is that the two layer forward model represents the lower dry firn contribution by the January to April mean SMAP brightness temperature. After the melt season, the snow and firn column may become dry again while retaining a different radiometric baseline because of refreezing, ice layer formation, or other microstructural changes. This occurs most clearly in the November part of the time series. In that situation, the observed TB can differ from the January to April reference even without liquid water. A two layer model can then fit the shifted dry baseline by assigning a small wet layer at the top. Such a solution is a numerical fit, not a physical wet snow state. The dry screening step is designed to identify and remove these weak wet solutions by using time series signatures that are not contained in the simple two layer fit alone.

7.2 Polarization and morning evening diagnostics

The screening uses the polarization difference and vertical to horizontal ratio,

$$\mathrm{PD}_i = \mathrm{TB}_{v,i}^{\mathrm{obs}} - \mathrm{TB}_{h,i}^{\mathrm{obs}}, \qquad \mathrm{VHR}_i = \frac{\mathrm{TB}_{v,i}^{\mathrm{obs}}}{\mathrm{TB}_{h,i}^{\mathrm{obs}}}. \tag{S51}$$

where $\mathrm{TB}_{v,i}^{\mathrm{obs}}$ and $\mathrm{TB}_{h,i}^{\mathrm{obs}}$ are the observed brightness temperatures. Dry snow tends to have a large and stable PD_i and NPR_i. During active melt, the polarization contrast often collapses and the evening pass can differ strongly from the morning pass.

For days with both morning and evening passes, the day scale diagnostics are

$$\mathrm{DAV}_d^{\mathrm{mean}} = \frac{1}{2}\left[(\mathrm{TB}_{v,e} + \mathrm{TB}_{h,e}) - (\mathrm{TB}_{v,m} + \mathrm{TB}_{h,m})\right], \tag{S52}$$

$$\mathrm{DAV}_d^{\mathrm{PD}} = \mathrm{PD}_m - \mathrm{PD}_e, \tag{S53}$$

$$\mathrm{DAV}_d^{\mathrm{NPR}} = \mathrm{NPR}_m - \mathrm{NPR}_e. \tag{S54}$$

where subscripts m and e denote morning and evening passes of the same day, PD is defined in Eq. (S51), and NPR is defined in Eq. (S14). Each diagnostic is converted into a positive dry referenced excess,

$$\mathcal{R}(x) = \mathrm{clip}_{[0,1]}\left[\frac{x - (\mu_{\mathrm{dry}} + z_0 s_{\mathrm{dry}})}{(z_1 - z_0)s_{\mathrm{dry}}}\right], \qquad z_0 = 1, \quad z_1 = 3, \tag{S55}$$

where μ_{dry} is the dry season median, $s_{\mathrm{dry}} = 1.4826\,\mathrm{MAD}$ is the robust dry season scale, and the clipping operator is defined in Eq. (S1). The diurnal melt indicator is

$$\mathcal{D}_i^{\mathrm{diurnal}} = \mathrm{clip}_{[0,1]}\left(0.20\mathcal{R}(\mathrm{DAV}^{\mathrm{mean}}) + 0.35\mathcal{R}(\mathrm{DAV}^{\mathrm{PD}}) + 0.45\mathcal{R}(\mathrm{DAV}^{\mathrm{NPR}})\right). \tag{S56}$$

where $\mathrm{DAV}^{\mathrm{mean}}$, $\mathrm{DAV}^{\mathrm{PD}}$, and $\mathrm{DAV}^{\mathrm{NPR}}$ are defined in Eqs. (S52) to (S54), and $\mathcal{R}(\cdot)$ is defined in Eq. (S55). The indicator is high when the day scale behavior resembles active melt.

7.3 Dry like polarization recovery and stability

Let $\mathrm{PD}_{\mathrm{hi}}$ and $\mathrm{PD}_{\mathrm{lo}}$ denote high and low seasonal polarization levels, and let $\mathrm{NPR}_{\mathrm{hi}}$ and $\mathrm{NPR}_{\mathrm{lo}}$ denote the corresponding NPR levels:

$$\mathrm{PD}_{\mathrm{hi}} = \max[P_{85}(\mathrm{PD}), \mathrm{PD}^{\mathrm{dry}}], \qquad \mathrm{PD}_{\mathrm{lo}} = \min[P_{15}(\mathrm{PD}), P_{25}(\mathrm{PD})], \tag{S57}$$

$$\mathrm{NPR}_{\mathrm{hi}} = \max[P_{85}(\mathrm{NPR}), \mathrm{NPR}^{\mathrm{dry}}], \qquad \mathrm{NPR}_{\mathrm{lo}} = \min[P_{15}(\mathrm{NPR}), P_{25}(\mathrm{NPR})]. \tag{S58}$$

where PD is defined in Eq. (S51), NPR is defined in Eq. (S14), and P_q denotes the qth percentile of the seasonal sequence.

The five pass stability indicators are

$$\mathcal{S}_i^{\mathrm{PD}} = 1 - \mathrm{clip}_{[0,1]}\left(\frac{\mathrm{std}_5(\mathrm{PD})_i - s_{\mathrm{PD},0}}{s_{\mathrm{PD},1} - s_{\mathrm{PD},0}}\right), \tag{S59}$$

$$\mathcal{S}_i^{\mathrm{NPR}} = 1 - \mathrm{clip}_{[0,1]}\left(\frac{\mathrm{std}_5(\mathrm{NPR})_i - s_{\mathrm{NPR},0}}{s_{\mathrm{NPR},1} - s_{\mathrm{NPR},0}}\right). \tag{S60}$$

where PD and NPR are defined in Eqs. (S51) and (S14). The operation std_5 is defined in Section 1.

The recovered polarization indicators are

$$\mathcal{R}_i^{\mathrm{PD}} = \mathrm{clip}_{[0,1]}\left(\frac{(\mathrm{PD}_i - \mathrm{PD}_{\mathrm{lo}})/(\mathrm{PD}_{\mathrm{hi}} - \mathrm{PD}_{\mathrm{lo}}) - r_{\mathrm{PD},0}}{r_{\mathrm{PD},1} - r_{\mathrm{PD},0}}\right), \tag{S61}$$

$$\mathcal{R}_i^{\mathrm{NPR}} = \mathrm{clip}_{[0,1]}\left(\frac{(\mathrm{NPR}_i - \mathrm{NPR}_{\mathrm{lo}})/(\mathrm{NPR}_{\mathrm{hi}} - \mathrm{NPR}_{\mathrm{lo}}) - r_{\mathrm{NPR},0}}{r_{\mathrm{NPR},1} - r_{\mathrm{NPR},0}}\right). \tag{S62}$$

where $\mathrm{PD}_{\mathrm{hi}}$ and $\mathrm{PD}_{\mathrm{lo}}$ are defined in Eq. (S57), and $\mathrm{NPR}_{\mathrm{hi}}$ and $\mathrm{NPR}_{\mathrm{lo}}$ are defined in Eq. (S58).

A large and stable polarization difference is represented as

$$\mathcal{B}_i^{\mathrm{PD}} = \mathrm{clip}_{[0,1]}\left(\frac{\mathrm{PD}_i - B_{\mathrm{PD},0}}{B_{\mathrm{PD},1} - B_{\mathrm{PD},0}}\right), \qquad \mathcal{B}_i^{\mathrm{PDstab}} = \sqrt{\mathcal{B}_i^{\mathrm{PD}}\mathcal{S}_i^{\mathrm{PD}}}. \tag{S63}$$

where PD_i is defined in Eq. (S51), and $\mathcal{S}_i^{\mathrm{PD}}$ is defined in Eq. (S59). The dry polarization evidence is represented compactly as

$$\mathcal{D}_i^{\mathrm{pol}} = \max\left(\mathcal{C}_i^{\mathrm{PD}}, \mathcal{B}_i^{\mathrm{PDstab}}, \sqrt{\mathcal{C}_i^{\mathrm{NPR}}\mathcal{S}_i^{\mathrm{NPR}}}, \mathcal{D}_i^{\mathrm{recov}}, \mathcal{D}_i^{\mathrm{tail}}, \mathcal{D}_i^{\mathrm{flat}}\right). \tag{S64}$$

where $\mathcal{B}_i^{\mathrm{PDstab}}$ is defined in Eq. (S63), and $\mathcal{S}_i^{\mathrm{NPR}}$ is defined in Eq. (S60). The terms $\mathcal{C}^{\mathrm{PD}}$ and $\mathcal{C}^{\mathrm{NPR}}$ measure closeness to the dry reference, $\mathcal{D}^{\mathrm{recov}}$ uses the recovery indicators in Eqs. (S61) and (S62), and $\mathcal{D}^{\mathrm{tail}}$ and $\mathcal{D}^{\mathrm{flat}}$ measure persistent late season flatness. Their thresholds are listed in Tables S6 and S7.

7.4 Dry and wet screening evidence

The onset evidence is used to avoid incorrectly removing genuine early melt:

$$\mathcal{E}_i^{\mathrm{onset}} = \mathrm{clip}_{[0,1]}\left(0.20\mathcal{D}_i^{\mathrm{diurnal}} + 0.16\mathcal{C}_i + 0.18\mathcal{C}_i^{\mathrm{rate}} + 0.12\mathcal{J}_i^{\mathrm{TB}} + 0.10\mathcal{G}_i^{d} + 0.08\mathcal{G}_i^{\mathrm{LWA}} + 0.16\mathcal{G}_i^{\mathrm{fit}}\right). \tag{S65}$$

where $\mathcal{D}_i^{\mathrm{diurnal}}$ is defined in Eq. (S56). The terms $\mathcal{C}_i$, $\mathcal{C}_i^{\mathrm{rate}}$, $\mathcal{J}_i^{\mathrm{TB}}$, $\mathcal{G}_i^{d}$, $\mathcal{G}_i^{\mathrm{LWA}}$, and $\mathcal{G}_i^{\mathrm{fit}}$ are normalized indicators of polarization collapse strength, polarization collapse rate, TB jump activity, retrieved depth growth, retrieved LWA growth, and wet fit improvement over dry fit, respectively. Their thresholds are listed in Tables S6 and S7.

The warm dry evidence is

$$\mathcal{E}_i^{\mathrm{warmdry}} = \mathrm{clip}_{[0,1]}\Big[0.20\mathcal{L}_i^{\mathrm{LWA}}\big(0.26\mathcal{D}_i^{\mathrm{pol}} + 0.18\mathcal{S}_i^{\mathrm{PD}} + 0.14\mathcal{S}_i^{\mathrm{NPR}} + 0.12(1 - \mathcal{D}_i^{\mathrm{diurnal}}) onumber \tag{S66}$$

$$+ 0.12\mathcal{G}_i^{\mathrm{dryfit}} + 0.18\mathcal{D}_i^{\mathrm{flat}}\big) + 0.15\mathcal{F}_i^{\mathrm{film}} + 0.35\max(\mathcal{L}_i^{\mathrm{tail}}, 0.45)\mathcal{D}_i^{\mathrm{post}}(1 - 0.45\mathcal{C}_i^{\mathrm{rate}}) onumber \tag{S67}$$

$$+ 0.30\mathcal{L}_i^{\mathrm{tailobs}}\mathcal{D}_i^{\mathrm{flat}}\Big]. \tag{S68}$$

where $\mathcal{D}_i^{\mathrm{pol}}$ is defined in Eq. (S64), $\mathcal{S}_i^{\mathrm{PD}}$ and $\mathcal{S}_i^{\mathrm{NPR}}$ are defined in Eqs. (S59) and (S60), and $\mathcal{D}_i^{\mathrm{diurnal}}$ is defined in Eq. (S56). The remaining symbols are normalized screening indicators: $\mathcal{L}^{\mathrm{LWA}}$ is low preliminary LWA, $\mathcal{G}^{\mathrm{dryfit}}$ is dry fit closeness, $\mathcal{D}^{\mathrm{flat}}$ is late season flatness, $\mathcal{F}^{\mathrm{film}}$ identifies high α, low LWC, shallow depth solutions, $\mathcal{L}^{\mathrm{tail}}$ and $\mathcal{L}^{\mathrm{tailobs}}$ are late season low LWA indicators, and $\mathcal{D}^{\mathrm{post}}$ indicates recovered dry behavior after melt.

The freeze dry evidence is

$$\mathcal{E}_i^{\mathrm{freezedry}} = \mathrm{clip}_{[0,1]}\big(0.14\mathcal{L}_i^{\mathrm{tail}} + 0.24\mathcal{D}_i^{\mathrm{post}} + 0.18\mathcal{D}_i^{\mathrm{tail}} + 0.18\mathcal{D}_i^{\mathrm{flat}} + 0.10\mathcal{S}_i^{\mathrm{PD}} onumber \tag{S69}$$

$$+ 0.06\mathcal{S}_i^{\mathrm{NPR}} + 0.10\max(\mathcal{G}_i^{\mathrm{dryfit}}, D_i^{\mathrm{fit}})\big). \tag{S70}$$

where $\mathcal{S}_i^{\mathrm{PD}}$ and $\mathcal{S}_i^{\mathrm{NPR}}$ are defined in Eqs. (S59) and (S60), and D_i^{fit} is defined in Eq. (S32). Other terms are normalized late season dry indicators described below Eq. (S68).

The final wet and dry memories are

$$\mathcal{M}_i^{\mathrm{wet}} = \max\left(\mathcal{E}_i^{\mathrm{onset}}, e^{-\Delta t_i/\tau_{\mathrm{wet}}}\mathcal{M}_{i-1}^{\mathrm{wet}}\right),$$
$$\mathcal{M}_i^{\mathrm{dry}} = \max\left(\mathcal{E}_i^{\mathrm{warmdry}}, \mathcal{E}_i^{\mathrm{freezedry}}, e^{-\Delta t_i/\tau_{\mathrm{dry}}}\mathcal{M}_{i-1}^{\mathrm{dry}}\right). \quad \text{(S71)}$$

where $\mathcal{E}_i^{\mathrm{onset}}$ is defined in Eq. (S65), $\mathcal{E}_i^{\mathrm{warmdry}}$ is defined in Eq. (S68), and $\mathcal{E}_i^{\mathrm{freezedry}}$ is defined in Eq. (S70). A pass is kept as wet when the onset or retention evidence is strong and is not overridden by persistent dry evidence. Otherwise it is classified as dry and the final reported wet variables are set to $\alpha = 0$, LWC $= 0$, $d_{\mathrm{wet}} = 0$, and LWA $= 0$.

8 Numerical parameter values

Table S1: Fixed retrieval and candidate grid settings.

Parameter	Value	Meaning
f	1.4 GHz	SMAP L band frequency
θ	40°	Incidence angle
ρ_s	400 kg m^{-3}	Fixed wet snow density
$d_{\mathrm{wet}}^{\mathrm{min}}$	0.03 m	Minimum wet layer thickness
$d_{\mathrm{wet}}^{\mathrm{max}}$	4.0 m	Maximum wet layer thickness
$d_{\mathrm{dry}}^{\mathrm{min}}$	0.02 m	Minimum dry fit upper layer depth
$d_{\mathrm{dry}}^{\mathrm{max}}$	30.0 m	Maximum dry fit upper layer depth
N_{LWC}	34	Coarse LWC grid points per candidate class
N_α	21	Coarse α grid points per candidate class
Candidates kept per class	6	Diverse best candidates retained
LWC diversity separation	0.003	Candidate diversity scale
α diversity separation	0.08	Candidate diversity scale
d diversity separation	0.20 m	Candidate diversity scale

Table S2: Local objective weights and normalization scales. The notation follows Eq. (S46).

Symbol or name	Value	Description
σ_T	2.0 K	TB residual scale
$w_{T,i}$	1.0 default	TB fit weight for most passes
$w_{T,1}$	2.2	TB fit weight at first pass
$w_{T,2}$	1.54	Minimum TB fit weight at second pass
$w_{T,3}$	0.99	Minimum TB fit weight at third pass
w_{adm}	0.34	Wet admission penalty weight
w_{dry}	0.46	Dry explanation penalty weight
w_{tail}	0.26	Late season LWA penalty weight
w_{stable}	0.42	Stable dry penalty weight
w_{drylike}	0.18	Dry like dielectric penalty weight
w_{high}	0.04	High LWC penalty weight

Symbol or name	Value	Description
w_α	0.02	α prior penalty weight
w_d	0.03	Wet depth prior penalty weight
w_{mode}	0.03	Candidate class prior penalty weight
w_{edge}	0.006	Edge penalty weight
w_{shape}	0.02	SMAP TB shape LWA penalty weight
w_{cap}	0.10	Depth cap penalty weight
σ_{adm}	0.16	Wet admission scale
σ_{drygain}	0.45	Dry fit gain scale
σ_{LWC}	0.010	LWC soft bound scale
σ_α	0.18	α prior scale
σ_d	0.32 m	Wet depth prior scale
q	6.0	Edge exponent
σ_{shape}	18.0 mm	LWA shape scale
σ_{tail}	2.5 mm	Tail LWA scale
σ_{cap}	0.08 m	Depth cap scale
$\sigma_{\alpha,\text{stable}}$	0.35	Stable dry α scale
$\sigma_{d,\text{stable}}$	0.22 m	Stable dry depth scale
$\sigma_{\text{LWA,stable}}$	2.5 mm	Stable dry LWA scale
σ_{drylike}	0.45	Dry like gain scale

Table S3: Dynamic programming weights and scales.

Parameter	Value	Description
ω_{local}	1.00	Local cost multiplier
ω_α	0.03	Jump penalty on α
ω_{LWC}	0.05	Jump penalty on LWC
ω_d	0.07	Jump penalty on d_{wet}
ω_{LWA}	0.05	Jump penalty on LWA
ω_m	0.04	Candidate class transition penalty
ω_{dir}	0.08	Directional LWA penalty
ω_{freeze}	0.14	Late season wet retention penalty
$\sigma_{\Delta\alpha}$	0.15	α jump scale
$\sigma_{\Delta\text{LWC}}$	0.008	LWC jump scale
$\sigma_{\Delta d}$	0.45 m	Wet depth jump scale
$\sigma_{\Delta\text{LWA}}$	14.0 mm	LWA jump scale
σ_{dir}	8.0 mm	Directional LWA scale
δ_{wet}	0.02	Wet evidence change tolerance
σ_{freeze}	2.5 mm	Freeze transition LWA scale

Table S4: Wet evidence and gate parameters.

Parameter	Value	Description
Smoothing window	1 pass	TB anomaly smoothing window

Parameter	Value	Description
A_0	3.0 K	Low anomaly threshold
High percentile	85	Percentile for anomaly normalization
η_0	0.012	Polarization departure lower threshold
η_1	0.035	Polarization departure upper threshold
Dry η exponent	1.35	Stable dry indicator exponent
Dry stability exponent	1.10	Stable dry indicator exponent
V^{TB} thresholds	1.0, 6.0 K	Local TB standard deviation thresholds
$V^{\Delta\mathrm{TB}}$ thresholds	0.8, 6.0 K	TB jump thresholds
V^{NPR} thresholds	0.002, 0.010	NPR variability thresholds
V_i weights	0.40, 0.35, 0.25	TB std, TB jump, NPR std weights
Entry weights	0.50, 0.20, 0.15, 0.15	η, rise, anomaly, variability
Wet weights	0.45, 0.25, 0.15, 0.15	η, memory, anomaly, variability
τ_M	8 days	Melt memory time scale
$\mathcal{W}_{\min}$	0.24	Wet admission required evidence
$G_{\min}$	0.60	Minimum wet fit gain over dry fit
$\mathrm{LWC}_{\mathrm{low}}$	0.006	Low water reference for dry like penalty
$\mathrm{LWC}_i^{\mathrm{soft}}$ base	0.001	Soft LWC reference base
$\mathrm{LWC}_i^{\mathrm{soft}}$ amplitudes	0.010, 0.008, 0.004	η, memory, variability amplitudes
LWA cap base	1.5 mm	Soft LWA cap base
LWA cap amplitude	9.0 mm	Soft LWA cap amplitude

Table S5: Wet layer depth reference parameters.

Parameter	Value	Description
$d_{\mathrm{wet}}^{\min}$	0.03 m	Minimum wet depth
$d_{\mathrm{wet}}^{\max}$	4.0 m	Maximum wet depth
d_i^{ref} base	0.04 m	Reference depth base
d_i^{ref} entry amplitude	0.22 m	Wet strength amplitude
d_i^{ref} memory amplitude	2.00 m	Melt memory amplitude
d_i^{hi} floor	0.08 m	Local high depth floor
d_i^{hi} entry amplitude	0.30 m	Wet strength amplitude
d_i^{hi} memory amplitude	2.15 m	Melt memory amplitude
d_i^{hi} η amplitude	0.40 m	Polarization departure amplitude

Table S6: Post retrieval dry screening thresholds.

Parameter	Value	Description
Low LWA range	4 to 10 mm	Low LWA indicator thresholds
Hard wet LWA	15 mm	Hard wet LWA threshold
Hard wet depth	0.35 m	Hard wet depth threshold
Low depth threshold	0.20 m	Shallow depth dry screen threshold
Low LWC threshold	0.006	Low LWC dry screen threshold
High α threshold	0.65	Film like weak wet threshold
NPR closeness scale	0.010	Dry reference NPR closeness
PD stability range	1.0 to 4.0 K	Moving window PD stability
NPR stability range	0.002 to 0.012	Moving window NPR stability
V/H ratio stability range	0.004 to 0.020	Moving window ratio stability
V/H ratio flat slope range	0.003 to 0.018	Ratio flatness
Ratio recovery fractions	0.52 to 0.72	Ratio recovery thresholds
TB jump range	3.0 to 12.0 K	TB jump activity thresholds
Depth growth range	0.05 to 0.30 m	Depth growth thresholds
LWA growth range	2.0 to 15.0 mm	LWA growth thresholds
PD large floor fraction	0.55	Large PD lower fraction of dry PD
PD large high fraction	0.90	Large PD upper fraction of dry PD
Default diurnal neutral	0.45	Diurnal value when no day pair exists
Wet fit gain range	0.18 to 1.00	Wet fit advantage thresholds
Dry fit closeness range	0.15 to 0.80	Dry fit closeness thresholds
Tail low LWA range	8 to 25 mm	Late season low LWA thresholds
PD recovery fractions	0.55 to 0.80	PD recovery thresholds
NPR recovery fractions	0.55 to 0.80	NPR recovery thresholds
PD drop rate range	2.0 to 10.0 K	Polarization collapse rate thresholds
NPR drop rate range	0.004 to 0.020	NPR collapse rate thresholds
Post dry fit gain maximum	0.45	Maximum wet advantage for post dry state
Onset fit gain minimum	0.25	Minimum wet advantage for onset

Table S7: Additional late season flatness and observational dry screening thresholds.

Parameter	Value	Description
PD flat slope range	0.8 to 3.5 K	PD flatness thresholds
NPR flat slope range	0.0015 to 0.0080	NPR flatness thresholds
Tail plateau threshold	0.70	Tail plateau dry threshold
Hard tail plateau threshold	0.86	Strong tail plateau threshold
TB stability range	1.4 to 6.0 K	TB level stability thresholds
TB flat slope range	0.8 to 3.2 K	TB flatness thresholds
Tail observed LWA range	10 to 32 mm	Observational tail LWA thresholds
Tail observed plateau threshold	0.68	Observational plateau threshold
Hard observed plateau threshold	0.84	Strong observational plateau threshold

Parameter	Value	Description
Tail observed diurnal maximum	0.35	Maximum diurnal melt for dry tail
Tail observed collapse maximum	0.45	Maximum polarization collapse for dry tail
Low relative TB fractions	0.32 to 0.58	Low TB relative level thresholds
Long flat look ahead	6 passes	Future window for long flat dry state
Long flat look back	6 passes	Past window for long flat dry state

Table S8: Final wet mask hysteresis parameters.

Parameter	Value	Description
τ_{wet}	3.0 days	Wet memory time scale
τ_{dry}	3.5 days	Dry memory time scale
Wet enter threshold	0.48	Main wet entry threshold
Wet enter seed threshold	0.30	Weak onset seed threshold
Strong wet enter threshold	0.60	Strong onset threshold
Wet entry fit gain minimum	0.22	Minimum wet fit advantage
Dry block fit gain threshold	0.20	Blocks weak wet entry under dry evidence
Keep wet threshold	0.20	Wet retention evidence threshold
Keep wet LWA	6.0 mm	LWA threshold for retaining wet state
Keep wet depth	0.18 m	Depth threshold for retaining wet state
Keep wet fit gain minimum	0.18	Wet fit advantage for retaining wet state
Dry exit threshold	0.58	Dry memory exit threshold
Minimum wet run	2 passes	Minimum accepted wet run length
Fill dry gaps	1 pass	Maximum dry gap filled inside wet run
Suspicious film threshold	0.55	High α, low water dry screen threshold
Onset backfill	2 passes	Maximum backward onset filling
Backfill seed threshold	0.22	Backfill onset evidence threshold
Backfill fit gain minimum	0.18	Backfill wet fit advantage
Backfill strong wet gain	0.40	Overrides weak dry film condition
Backfill collapse rate threshold	0.28	Collapse rate threshold for backfill
Backfill jump threshold	0.25	TB jump threshold for backfill
Backfill depth minimum	0.08 m	Depth threshold for backfill
Backfill LWA minimum	5.0 mm	LWA threshold for backfill
Post dry recovered threshold	0.72	Recovered dry polarization threshold
Post dry fit gain maximum	0.45	Maximum wet advantage for post dry
Post dry LWA maximum	25.0 mm	Maximum LWA for post dry classification
Post dry diurnal maximum	0.28	Diurnal threshold for post dry

Parameter	Value	Description
Post dry collapse maximum	0.45	Collapse threshold for post dry
Post dry collapse rate maximum	0.35	Collapse rate threshold for post dry
Tail wet retain maximum	0.50	Tail wet retention maximum
Post dry plateau threshold	0.72	Plateau dry threshold
Hard post dry plateau threshold	0.86	Strong plateau dry threshold
Strong post dry diurnal maximum	0.35	Strong dry tail diurnal limit
Strong post dry collapse maximum	0.42	Strong dry tail collapse limit
Strong post dry collapse rate maximum	0.32	Strong dry tail collapse rate limit
Hard tail wet retain plateau maximum	0.85	Plateau override for retained wet state
Observed post dry plateau threshold	0.70	Observational plateau threshold
Hard observed post dry plateau threshold	0.84	Strong observational plateau threshold
Observed post dry diurnal maximum	0.35	Observational post dry diurnal limit
Observed post dry collapse maximum	0.45	Observational post dry collapse limit
Observed post dry LWA threshold	0.28	Observed tail LWA threshold
Observed tail wet retain plateau maximum	0.82	Observational plateau override

9 Interpretation of the tuning parameters

The weights w and ω and the normalization scales σ in this Supplementary Information are not additional physical parameters of wet snow. They are numerical regularization parameters used to stabilize an underdetermined inverse problem. The direct TB misfit in Eq. (S29) remains the primary local constraint. The other terms help select a physically coherent seasonal path, suppress artificial weak wet solutions in dry periods, and avoid edge solutions that are not well supported by the retrieval model. The dry screening thresholds serve a similar role: they identify cases where the preliminary wet solution is mainly explaining a shifted dry baseline rather than true liquid water.

10 Representative sensitivity and ablation test

This section adds a compact sensitivity test to evaluate whether the main retrieval behavior depends strongly on one particular regularization choice. The purpose is not to produce a complete uncertainty quantification. Instead, the test is designed to address three questions: whether the post retrieval dry screening is necessary, whether the weak SMAP TB shape guide forces the retrieved

LWA seasonal pattern, and whether the results are strongly dependent on the exact numerical values of the regularization weights.

The test is performed for the CP1 morning pass retrieval because this site contains a clear melt onset, a strong main melt period, and a post melt period in which the dry brightness temperature baseline is shifted relative to the January to April reference. The same retrieval framework, forward model, neural network permittivity emulator, candidate library, and input observations are used in all cases. Only the specific regularization or screening choice described below is changed.

The five cases shown in Fig. S1 are defined as follows.

1. **Baseline.** This is the standard retrieval used in the main paper. It includes the wet first time series inversion, the weak SMAP TB shape LWA regularization term in Eq. (S30), the dynamic programming transition cost in Eq. (S49), and the post retrieval dry screening described in Sect. 7. Dry passes identified by the dry screening are assigned final wet variables equal to zero.

2. **No dry screen.** In this ablation case, the post retrieval dry screening is removed. The preliminary wet first time series path is used directly as the final retrieval, so no pass is overwritten by the dry solution after the wet first step. All forward model settings, local cost terms, dynamic programming weights, and candidate libraries are otherwise unchanged. This case is intended to test the role of the dry screening. If the two layer model interprets a shifted post melt dry baseline as a small wet layer, this case should retain weak nonzero LWA or wet layer thickness after the true melt season has ended.

3. **No TB shape prior.** In this ablation case, the weak SMAP TB shape LWA regularization is removed by setting the corresponding local cost weight to zero,

$$w_{\text{shape}} = 0, \tag{S72}$$

   where w_{shape} is the weight multiplying $J_{i,j}^{\text{shape}}$ in Eq. (S46). All other weights, dry screening thresholds, dynamic programming settings, and physical forward model parameters are kept at their baseline values. This case tests whether the main LWA seasonal evolution is imposed by the TB shape term or whether it is mainly constrained by the two polarization TB fit and the temporal path selection.

4. **Weights -50%.** In this perturbation case, the main weak regularization weights in the local objective and the temporal coupling weights in the dynamic programming transition cost are multiplied by 0.5. Specifically, the local regularization weights associated with wet admission, dry explanation, late season LWA, stable dry behavior, dry like dielectric behavior, high LWC, α prior, depth prior, mode prior, edge, TB shape, and depth cap penalties are scaled by 0.5. The temporal coupling weights on jumps in α, LWC, d_{wet}, LWA, candidate class switching, directional LWA consistency, and late season wet retention are also scaled by 0.5. The direct TB residual scale σ_T, the physical forward model, the candidate grid, the neural network emulator, and the dry screening thresholds are not changed.

5. **Weights +50%.** This case is the same as the previous perturbation test, except that the same set of local regularization and temporal coupling weights are multiplied by 1.5. The direct TB residual scale, physical parameters, candidate grid, and dry screening thresholds are again unchanged. This case tests whether strengthening the regularization by a moderate amount changes the main seasonal interpretation.

The comparison in Fig. S1 supports three points. First, the baseline and the no TB shape prior case are very similar during the main melt season, especially for LWA and d_{wet}. This indicates

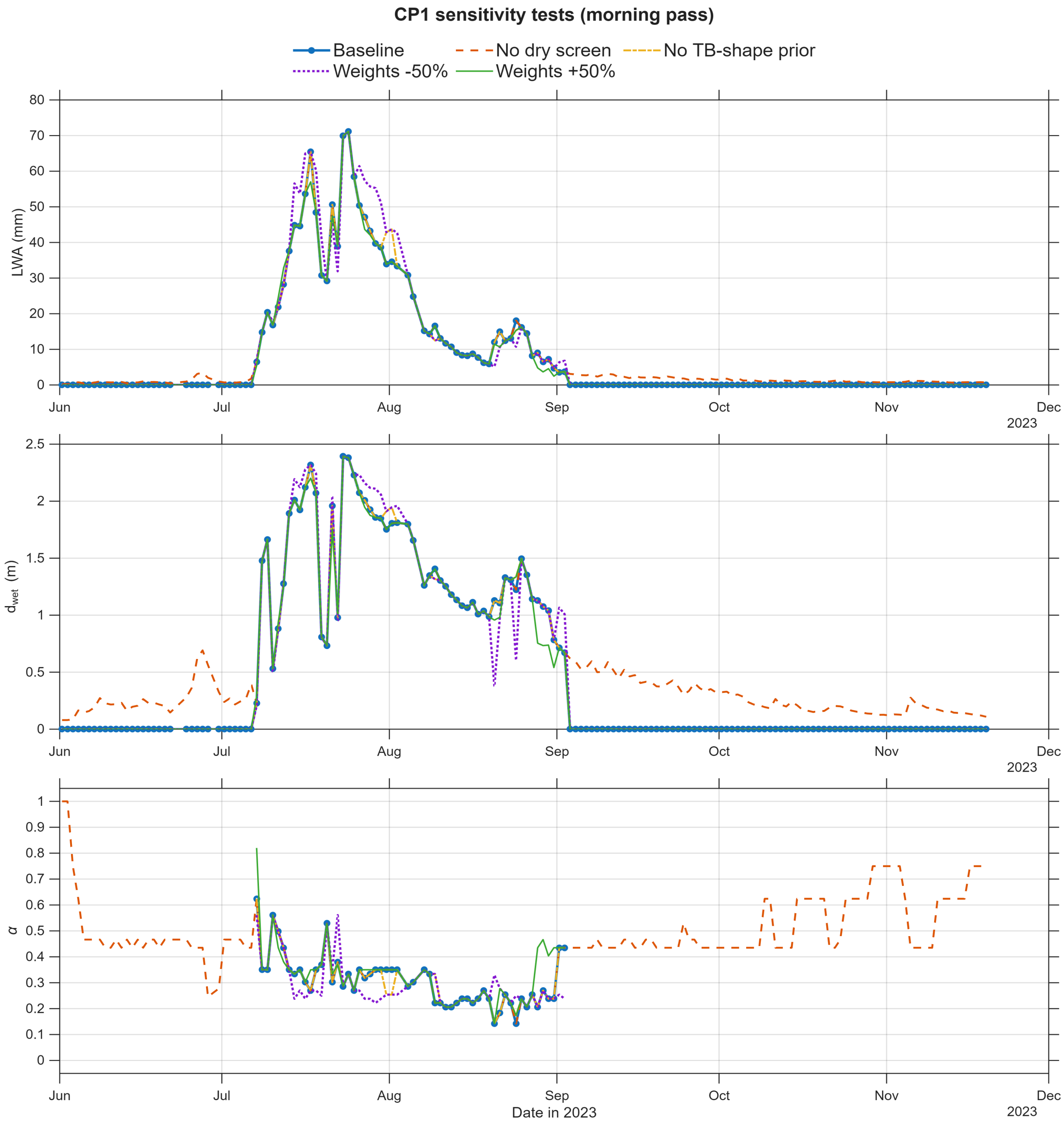

Figure S1: Sensitivity of the CP1 retrieval to dry screening, the weak SMAP TB shape regularization, and the main regularization weights. The baseline retrieval is compared with four ablation or perturbation cases: no post retrieval dry screening, removal of the weak SMAP TB shape prior, and ±50% changes to the main regularization and temporal coupling weights.

that the weak SMAP TB shape term helps guide the time series but does not by itself impose the retrieved seasonal LWA pattern. Second, multiplying the main regularization and temporal coupling weights by 0.5 or 1.5 preserves the timing of melt onset, the main peak, the broad LWA magnitude, and the seasonal evolution of d_{wet}. Thus, the main interpretation is not sensitive to the exact values of the regularization weights. Third, the no dry screen case behaves differently after the main melt season. It retains a shallow weak wet layer and non physical α values during the post melt period when the baseline retrieval has already returned to dry conditions. This is the behavior expected when the simplified two layer model tries to fit a shifted dry brightness temperature baseline by assigning a small amount of liquid water to the upper layer. The sensitivity test therefore supports the use of the post retrieval dry screening described in Sect. 7.

The α values in the dry or nearly dry part of the no dry screen case should not be interpreted as physical water morphology. They are shown only to illustrate the artificial weak wet solutions that appear when the dry screening step is removed. In the baseline retrieval, once a pass is classified as dry, the final reported wet variables are set to $\alpha = 0$, $\mathrm{LWC} = 0$, $d_{\mathrm{wet}} = 0$, and $\mathrm{LWA} = 0$.